International Symposium
On Turbulence and Shear Flow
Phenomena (TSFP-9)
June 30 - July 3, 2015 *Melbourne, Australia*

ON THE INFLUENCE OF COMPUTATIONAL DOMAIN LENGTH ON TURBULENCE IN OSCILLATING PIPE FLOW

Daniel Feldmann and Claus Wagner
Institute of Aerodynamics and Flow Technology
German Aerospace Center (DLR)
Bunsenstraße 10, 37073 Göttingen, Germany
daniel.feldmann@dlr.de

ABSTRACT

Here we present results from DNS of oscillating pipe flow at $Re = 11500$ and $Wo = 13$ using a fully developed turbulent flow field as initial condition and different length of the computational pipe domain. We found that the flow is conditionally turbulent for short and medium pipe domains, while the flow field completely laminarises in longer computational domains. This observation is discussed in more detail by comparing spatial power spectra, turbulence statistics and integral quantities of the resulting flow fields. We conclude that the critical maximum pipe length for this special scenario lies within $3.54D < L < 5D$.

INTRODUCTION

In turbulent shear flows large scale coherent structures play an important role since they contribute significantly to the momentum transport processes. They have to be resolved properly by the size of the computational domain. Especially when direct numerical simulation (DNS) techniques in conjunction with periodic boundary conditions in one or more coordinate directions are employed to investigate the underlying flow physics it is of utmost importance to choose a large enough computational domain. From DNS of statistically steady turbulent flow in pipe and channel geometries, it is well know that, a minimum domain size is required to maintain turbulence and prevent the flow from strong local or global laminarisation, see e.g. Jiménez & Moin (1991). Here, we present results from DNS of purely oscillating pipe flow; i.e. the flow periodically accelerates, reaches a peak value, decelerates and entirely reverses its direction in such a way, that there is no net mean flow through the pipe. We discuss the contrary finding, that turbulence in the oscillating flow field is damped and amplified repeatedly when using a relatively short pipe domain, while on the other hand the flow laminarises entirely when a longer computational domain is used. To our knowledge, there are only a few studies investigating purely oscillating flows numerically in general; i.e. flat plate, channel or pipe domains. And none of these studies have addressed the influence of the computational domain length on resulting flow field before.

THEORETICAL BACKGROUND

We consider a Newtonian fluid confined by a straight pipe of diameter D and length L. The fluid is driven in axial direction (z) by a time dependent mean pressure gradient

$$P(t) \equiv \left[0,0,\frac{d\langle p\rangle_\phi}{dz}\right]^\mathsf{T} = \left[0,0,-4\cos\left(\frac{4Wo^2}{Re_\tau}t\right)\right]^\mathsf{T}, \qquad (1)$$

where $p = p' + \langle p\rangle_\phi$ according to Reynolds' decomposition. Here, a prime denotes the fluctuating part of any quantity and angle brackets denote an averaging operation over time instants of equal oscillation phases ϕ. In the remainder of this paper there also appear angle brackets with other subscripts, which denote the particular averaging operation, e.g. t for averaging in time. Normalisation and the set of non-dimensional control parameters is given by the Womersley number $Wo = \tilde{D}/2\sqrt{\tilde{\omega}/\tilde{\nu}}$ and the friction Reynolds number $Re_\tau = \langle\tilde{u}_\tau\rangle_t \tilde{D}/\tilde{\nu}$. Here, $\tilde{\omega} = 2\pi/\tilde{T}$ is the forcing frequency, $\tilde{\nu}$ is the kinematic viscosity of the fluid, and $\langle\tilde{u}_\tau\rangle_t$ is the friction velocity of a fully developed statistically steady turbulent pipe flow at $Wo = 0$. The tilde denotes dimensional quantities. Thus, the governing equations in non-dimensional form read

$$\nabla\cdot u = 0 \quad \text{and} \quad \frac{\partial u}{\partial t} + (u\cdot\nabla)\,u + \nabla p' - \frac{1}{Re_\tau}\Delta u = P(t) \qquad (2)$$

with u denoting the velocity vector and ∇ and Δ being the Nabla operator and the Laplacian, respectively. Eqs (1) and (2) are supplemented by periodic boundary conditions (BC) for u and p' in the homogeneous directions z and φ and no-slip and impermeability BC at $r = D/2$ in the radial direction.

For a laminar, axially symmetric and fully developed (periodic) flow, a closed-form solution to eqs (1) and (2) for the axial velocity u_z exists, which was first derived by Sexl (1930) and later by Womersley (1955). Neutral curves resulting from linear stability analysis (Trukenmüller (2006), Thomas *et al.* (2012)) for this so-called Sexl-Womersley (SW) flow are shown in figure 1 together with experimental findings (Hino *et al.* (1976), Zhao & Cheng (1996),Eckmann & Grotberg (1991)) for the critical values separating the parameter space in laminar and different turbulent regimes. The regimes determined experimentally are not entirely consistent and there is also a huge discrepancy among the results from linear stability analysis. Here, the Reynolds number $Re = u_\mathrm{p} D/\nu$ is based on the amplitude of the bulk velocity $u_\mathrm{p} = \max u_\mathrm{b}(t)$ within $0 \le t < T$, which is a result for a given combination of the two control parameters Re_τ and Wo. Fig. 1 also shows the analytical relation

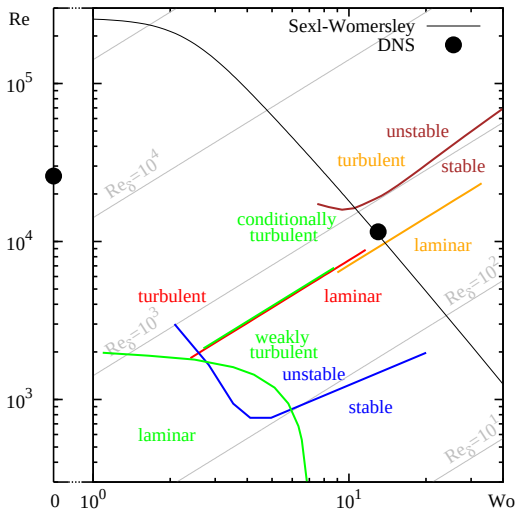

Figure 1. Parameter space for oscillating pipe flow. Different flow regimes according to experimental findings (Hino, Zhao, Eckmann) and linear stability analysis (Trukenmüller, Thomas).

between Re and Wo for a given $Re_\tau = 1440$, i.e. a given pressure gradient. One can easily see, that the peak velocity decreases with increasing oscillation frequency for a given forcing amplitude. Most of the experimentalists mentioned above have used the Reynolds number based on the Stokes layer thickness $\delta = \sqrt{2\nu/\omega}$ to characterise the flow, which is given by $Re_\delta = u_p\delta/\nu = Re/(\sqrt{2}Wo)$.

NUMERICAL APPROACH

In our DNS, a discrete form of eqs (1) and (2) is integrated by means of a fourth order accurate finite volume method and advanced in time using an explicit second order accurate leapfrog-Euler time integration scheme. Further details on the numerical method are given in Feldmann & Wagner (2012) and references therein.

For all DNS presented here, we first generated a well correlated statistically steady turbulent pipe flow at $Re_\tau = 1440$ and $Wo = 0$ in the respective pipe domain, which served as initial conditions for the oscillating pipe flow. Table 1 gives detailed information on the length of the used computational domain and its spatial discretisation. The variable time step is adapted according to von Neuman stability criterion and is always smaller than 1.1×10^{-5}. As discussed in Feldmann & Wagner (2012), both, the grid spacing and the time step is sufficiently small to resolve all relevant turbulent scales in case of the fully developed pipe flow at $Re_\tau = 1440$, which corresponds to $Re = 25960$.

In case of a fully-developed pipe flow at $Re_\tau = 1440$ and $Wo = 0$ the used pipe length correspond to values from $L^+ = 1700$ up to 10210 scaled in wall units. As discussed in Feldmann & Wagner (2012) and also known from Eggels *et al.* (1994), $L^+ = 1800$ should be sufficiently long to reproduce at least the integral quantities and the first statistical moments of the turbulent pipe flow in good accordance with results from DNS in longer computational domains and in accordance with experimental results. In the oscillating case at $Wo = 13$, the length of the used pipe domains correspond to values from $L = 22\delta$ up to 130δ, scaled in Stokes layer thicknesses. These values are comparable to the computational domain length used by other investigators to study similar flow problems numerically. Vittory & Verzicco (1998) and Spalart & Baldwin (1989) considered the oscillating boundary layer flow over a flat plate, and used computational domains of length $L = 13\delta$ and $L = 60\delta$, respectively. Akhavan *et al.* (1991) performed two-dimensional numerical simulations of the oscillating flow in a channel domain of length $L = 200\delta$.

RESULTS

For all performed DNS, the control parameters are $Re_\tau = 1440$ and $Wo = 13$. The mean pressure gradient given by eq. (1) starts to vary periodically at $t = 0$. As a result an oscillatory flow through the pipe develops from the initially turbulent and non-oscillating flow field within the first few forcing cycles. This can be seen from the time series of the bulk velocity plotted in fig. 2 for the shortest and the longest pipe domain. For $t > 26.8$ the amplitude of the resulting bulk flow is roughly half the value of the non-oscillating case with constant forcing, cf. fig.1. This is because the pressure gradient has to balance not only the shear forces at the wall but also the inertial forces related to the unsteady bulk flow. The temporal evolution of u_b is similar for all considered pipe domains and coincides quite well with the theoretical prediction of the bulk velocity $u_{b,SW}$ in terms of phase, amplitude and wave form. Thus, the resulting oscillatory pipe flows are all characterised by $Re \approx 11500$ and $Re_\delta = 630$, respectively. This is well above the critical value of $Re_\delta = 550$ found experimentally by Eckmann & Grotberg (1991) for the occurrence of turbulence, see fig. 1. In terms of the linear stability analysis performed by Thomas *et al.* (2012) based on Floquet-Theory, the SW flow is stable to general perturbations for this combination of Re and Wo. According to Trukenmüller (2006), who used a quasi-steady formulation of the linear stability problem, the SW flow is unstable at this point in the parameter space.

Fig. 2 also shows time series of the axial velocity component (u_z), which reveal major differences in the oscillating flow field when comparing the DNS results for the shortest and the longest pipe domain. Within the first three oscillation periods the flow in the longest pipe laminarises and does not become turbulent again. This is also reflected by the temporal evolution of azimuthal (u_φ) and the radial (u_r) velocity component, see fig. 2. The kinetic energy content in u_φ and u_r decays over many oscillation periods (not all plotted here). On the other hand, the kinetic energy content in u_φ and u_r repeatedly increases in accordance with the appearance of turbulent burst visible in the axial velocity time series taken from the DNS in the shortest pipe domain.

We found that in our DNS all the flow fields show qualitatively the same turbulent behaviour for the three shorter computational domains. For the two longer ones, the flow laminarises entirely. From this we conclude, that a critical maximum domain length which is needed to maintain turbulence in a DNS of oscillating pipe flow at this particular point in the parameter space lies between $3.54D$ and $5D$, see tab. 1.

Fig. 3 exemplarily shows time series of u_z in more detail at several radial positions for one full cycle, to give a better impression of the amplification and decay of the velocity fluctuations in the oscillating pipe flow. During phases of acceleration (AC) and peak flow (PF) the time signal is characterised by small fluctuations almost every-

Table 1. Setup of performed DNS. Computational domain length L in different scaling and the respective spatial discretisation in wall units (Plus) and number of grid points N. Number of samples for phase averaging N_ϕ and final flow state.

L/D	L/δ	L^+	Δz^+	$r^+\Delta\varphi\vert_{r=D/2}$	$\Delta r^+\vert_{r=0}$	$\Delta r^+\vert_{r=D/2}$	$N_z \times N_\varphi \times N_r$	N_ϕ	
1.18	22	1700	6.6	4.4	0.5	6.6	$256 \times 1024 \times 222$	8	cond. turb.
1.25	23	1800	7.0	4.4	0.5	11	$256 \times 1024 \times 128$	10	cond. turb.
3.54	65	5100	6.6	4.4	0.5	6.6	$768 \times 1024 \times 222$	5	cond. turb.
5.00	92	7200	7.0	4.4	0.5	11	$1024 \times 1024 \times 128$		laminar
7.09	130	10210	6.6	4.4	0.5	6.6	$1536 \times 1024 \times 222$		laminar

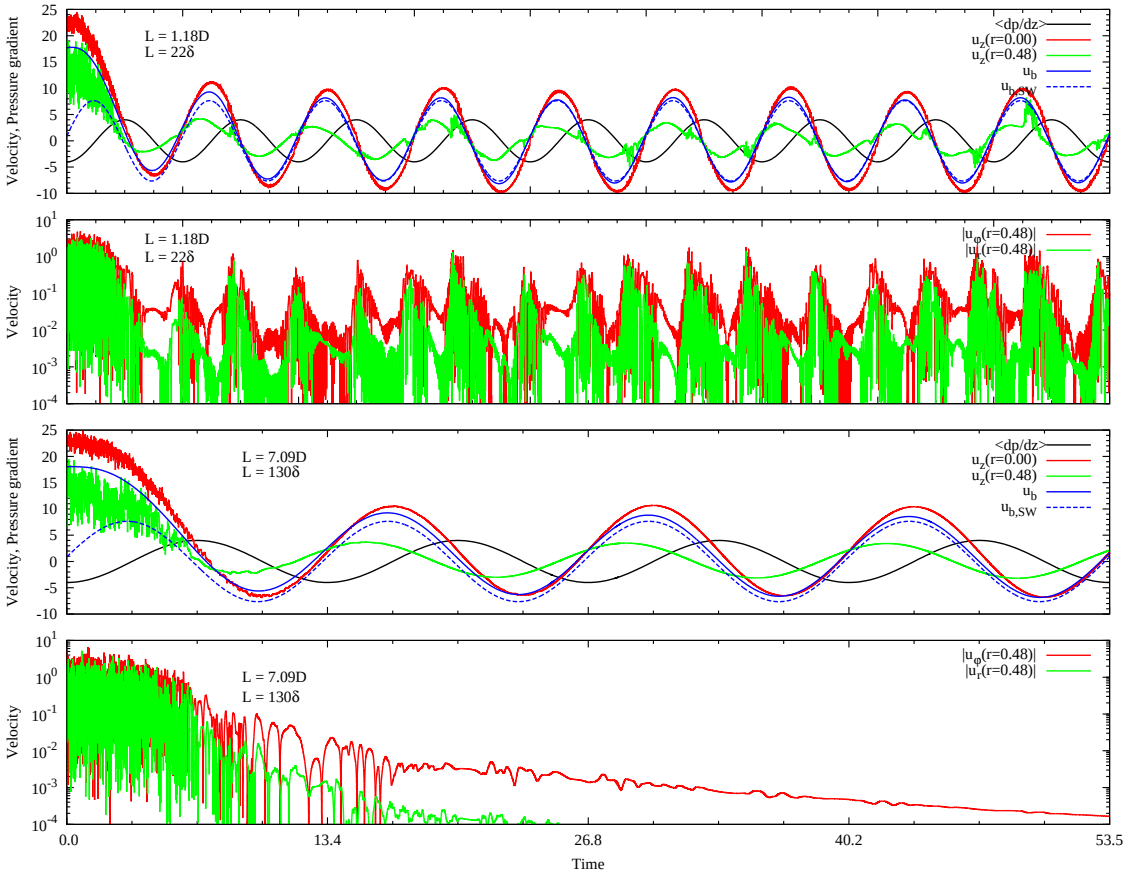

Figure 2. Temporal evolution of the bulk velocity and the axial (u_z), the azimuthal (u_φ), and the radial (u_r) velocity component at the pipe axis ($r = 0$) and close to the pipe wall ($r = 0.48$) in oscillating pipe flow at $Wo = 13$ and $Re \approx 11500$ as obtained by DNS. Shown are results for the shortest and for the longest computational pipe domain we considered, see tab. 1.

where in the pipe and it is rather smooth very close to the wall. During phases of deceleration (DC), these fluctuations are amplified. This leads to a turbulent burst and an abrupt breakdown of the smooth near wall flow. The generated fluctuations are damped again in the following phase of bulk flow acceleration (AC). This behaviour of the oscillating pipe flow is in very good overall agreement with most of the qualitative descriptions in the above mentioned experimental and numerical studies.

To quantify the influence of the used computational domain length, we compare the integral quantities of the resulting flow fields as a first step. Fig. 4 reveals that there is almost no influence of the domain length on the bulk velocity and the wall shear stress, when the resulting flow field is conditionally turbulent; i.e. $L \in \{1.18, 1.25, 3.54\}D$. The only difference is that during DC ($0.3T$ and $0.8T$), when the turbulent bursts occur, the wall shear stress is slightly higher for $L = 1.18D$ and $1.25D$ compared to $3.54D$. This indicates that the intensity of the turbulence which is generated during DC decreases with increasing domain length. A trend that leads to total laminarisation for even longer pipe domains. The bulk flow and the wall shear stress compares favourably with the predictions from theory (SW), when the resulting flow field is laminar; i.e. $L \in \{5.0, 7.09\}D$. This shows also, that for a given combination of Re_τ and Wo a turbulent version of this flow reaches a 4.5 % higher peak

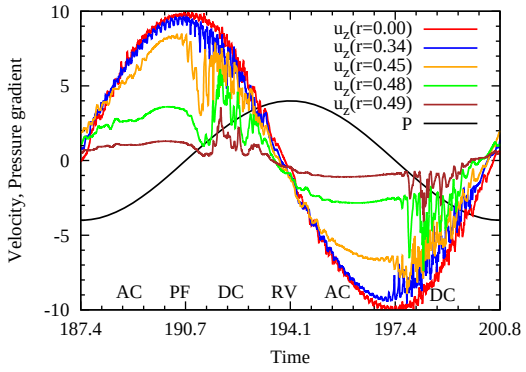

Figure 3. Time signal for u_z at several radial positions for $14T < t < 15T$ as obtained by DNS using a computational domain length of $L = 1.25D$. The forcing $P(t)$ is shown for orientation.

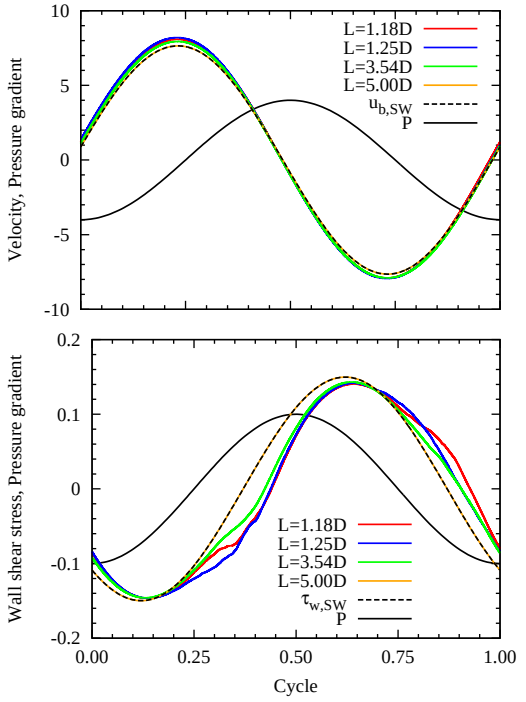

Figure 4. Temporal evolution of $\langle u_b \rangle_\phi$ and $\langle \tau_w \rangle_\phi$ averaged over several oscillation cycles for $t > 26.8$ as obtained by DNS for different length of the computational domain. The evolution of the forcing and the resulting bulk velocity according to the laminar theory (SW) is shown as reference.

flow rate at a 4.8 % lower level of wall shear stresses, compared to a laminar version of the flow in the same system.

Fig. 5 compares the mean velocity profiles at DC, RV, and AC. When the flow is laminar, the velocity profiles compare favourably with the predictions from theory (SW). The typical near wall peaks and inflection points in the radial distribution of the axial velocity component are reproduced for all phases of the oscillation cycle. When the flow is conditionally turbulent, there are major deviations in the mean velocity profiles compared to SW flow. In this case, the typical phase lag between the far and near wall

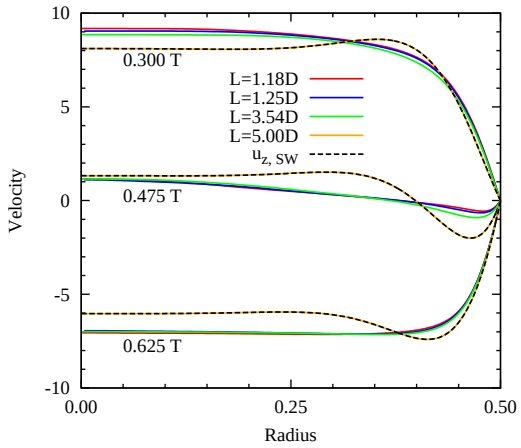

Figure 5. Radial profiles of $\langle u_z \rangle_{z,\varphi,\phi}$ averaged in the homogeneous spatial directions and over several oscillation cycles for $t > 26.8$ as obtained by DNS. The laminar theory (SW) is shown as reference for the three different instants during one oscillation cycle; i.e. DC, RV, and AC.

flow, which is a viscous effect, is strongly reduced by the turbulent fluctuations in the velocity field and the related enhancement of wall normal momentum transport.

Comparing the conditionally turbulent cases shows that the pipe length has almost no influence on the mean velocity profiles either. However, during AC the mean velocity profiles obtained for different pipe length are more similar compared to the velocity profiles during DC and RV Thus there is a minor dependency on the pipe length during phases of higher turbulence intensities and almost no dependency during phases of lower turbulence intensities. This differences can also be explained by different sizes of statistical samples used to compute the phase averaged profiles, see tab. 1. The longer the domain, the less simulated oscillation cycles are available for averaging due to enormous computational costs. For the longer domains, e.g. $L = 3.54D$, the grid consists of 1.5×10^7 grid points and for one period around 8.6×10^4 time integration steps has to be computed. This means that approximately 37 000 CPU hours are necessary to simulate one single cycle of the oscillating flow and thus, to improving the phase average by only one sample.

Fig. 6 compares profiles of the RMS velocity fluctuations for the three conditionally turbulent cases at DC, RV, and AC. The RMS profiles of the azimuthal velocity component are similar for all pipe length at all phases. Thus the length of the computational domain has only minor effects on the strength of the azimuthal velocity fluctuations. Fig. 6 also reveals, that azimuthal velocity fluctuations have a broad maximum in the near wall region during DC, when the turbulent bursts occur. During AC the azimuthal velocity fluctuations are damped only near the wall. On the other hand, the RMS profiles of the axial velocity component show a strong dependency on the used computational domain length. During DC, there is a distinct maximum very close to wall, which is typical for all turbulent wall bounded shear flows. The longer the pipe domain, the lower is the value of this maximum. At AC the near wall maximum is still present, but clearly decreased in accordance with the azimuthal RMS profiles. In the bulk region of the pipe, the axial RMS velocity fluctuations increase from DC

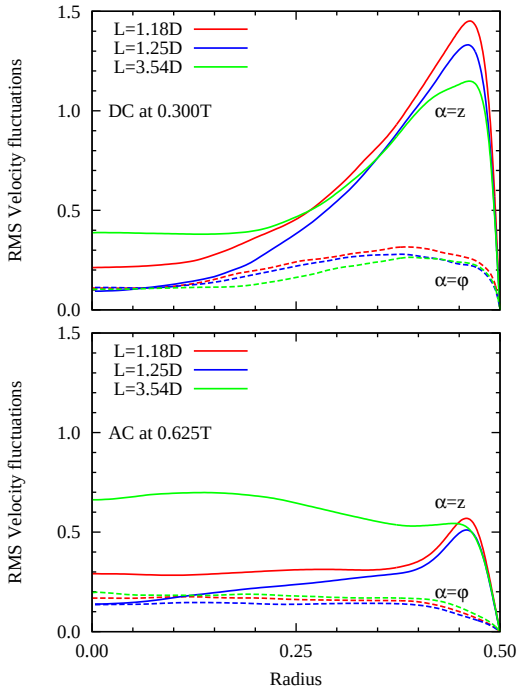

Figure 6. Radial profiles of $\langle u'_\alpha \rangle^{1/2}_{z,\varphi,\phi}$ as obtained by DNS for different length of the computational domain at two different instants during one oscillation cycle; i.e. DC and AC. Profiles for $\alpha = r$ (not shown) are similar to those for $\alpha = \varphi$.

to AC. This increase becomes more prominent with increasing domain length.

Fig. 7 compares power density spectra $E_{z\alpha}(k)$ obtained from one dimensional velocity signals $u_\alpha(z_i)$ in axial direction z. The energy spectra are calculated via

$$E_{z\alpha}(k) = |\hat{u}_\alpha(k)|^2 \quad \text{for} \quad k = 0, \ldots, {}^{N_z}/_2 \tag{3}$$

$$\text{with} \quad \hat{u}_\alpha(k) = \frac{1}{N_z} \sum_{i=0}^{N_z-1} u_\alpha(z_i) \cdot e^{(-j2\pi ik/N_z)} \tag{4}$$

being the discrete Fourier transform of the respective velocity signal and j denoting the imaginary unit. To plot the energy spectra, the angular wavenumber $\kappa_z = {}^{2\pi k}/_L$ is used as abscissa. The signals were taken at $r = 0.48$, approximately where the near wall peak occurs in the RMS profiles, see fig. 6. As a reference, fig. 7 shows energy spectra for the fully developed turbulent pipe flow at $Wo = 0$ and constant forcing P, which we used as initial condition for the DNS of oscillating flow at $Wo = 13$. The resulting Reynolds number of $Re = 25960$ for this case is too low and the location too close to the wall to expect an extensive inertial subrange, in which the energy content typically scales like to the power of $-5/3$ with the wavenumber κ_z. Although there is a small wavenumber range, where such a scaling is present, the plotted slope rather serves as a guideline to the eye to distinguish between the energy containing range of wavenumbers, i.e. a slope flatter than $-5/3$, and the dissipative range of wavenumbers, i.e. a slope steeper than $-5/3$. The lowest angular wavenumbers plotted in fig. 7, correspond to a wave length equal to the computational domain length; $\lambda_z = {}^{2\pi}/_{\kappa_z} = 7.09D$ in this case. The highest angular wavenumber, $\kappa_z \approx 700$, represents twice the grid spacing in axial direction, which is given in tab. 1. First of all, the steep decay of the kinetic energy content down to very small values below 10^{-8} at $\kappa_z \approx 600$ supports the statement, that the used spatial discretisation is sufficiently fine to resolve all relevant energy containing length scales in the dissipative range of the flow field at $Re = 25960$.

For the oscillating case with $Wo = 13$, the resulting peak Reynolds number is only $Re \approx 11500$ and thus the computational grid is even more adequate. During DC of the bulk flow, when fluctuations in the flow field are generated and amplified (only for those with $L \leq 3.54D$), the shape of the energy spectra compare well to the fully developed reference case. This is an evidence for the flow being turbulent during this period of the oscillation cycle. There is a steep decay in the energy spectrum for high wavenumbers and a small inertial subrange. The latter is more pronounced in the energy spectra for the axial velocity component as in those for the azimuthal ones. Nevertheless, the spectra for the DC phase are substantially shifted downwards to lower energy contents, compared to fully developed reference case. This can be explained by two facts. First, the resulting peak Reynolds is much lower. Second, the DC phase is too short to let the flow reach a fully developed turbulent state.

After DC and RV, the acceleration of the bulk flow has a stabilising effect and the fluctuations in the velocity field are damped substantially. This can be seen by comparing the energy spectra for AC and DC. Almost the entire spectrum has a very steep slope, which indicates that the flow is laminar and all the energy is dissipated by viscous mechanisms. Moreover, the forcing term $P(t)$ and thus the energy input to the flow, starts decrease during AC, which promotes the ongoing laminarisation.

Comparing the energy spectra for different computational domain length reveals major differences in the distribution of the kinetic energy. It is obvious that, a longer pipe domain allows the flow to develop larger energy containing structures. This, in turn, leads to a reduction of the energy content in the smaller wavelength, i.e. higher wavenumbers, during DC. To explain why the shorter pipe domains maintain a conditionally turbulent state in our DNS, while the flow laminarises entirely in the longer ones, we suggest to extrapolate this trend seen for $1.25D$ and $L = 3.54D$ to longer pipes. Since the SW flow is, according to Thomas *et al.* (2012), linearly stable for this set of parameters, it is likely that a certain amount of energy content in the small and medium wave length is necessary to trigger the transition to a turbulent state at this phase of the oscillation cycle. If the energy content in the higher wavenumber range is to too small at the beginning of any DC phase, the remaining disturbances in the flow are too weak to trigger a new transition to turbulence in the numerical simulations of the flow. Following this rationale, there has to be a critical domain length, below which the amount of energy trapped in smaller wavelength is still large enough to trigger the transition process. This hypothesis is supported by the spectra for longest pipe domain, which reveal a much lower energy content in smaller wavelengths at the DC and AC phase, after the first RV.

Further, for the cases where a conditionally turbulent state is maintained, the larger structures seem to survive longer, which can be seen by comparing the spectra at DC and AC for $L = 3.54D$ and $1.25D$. The energy content in the largest scales is almost the same at DC and AC in the longer pipe domain, while there is an substantial drop of

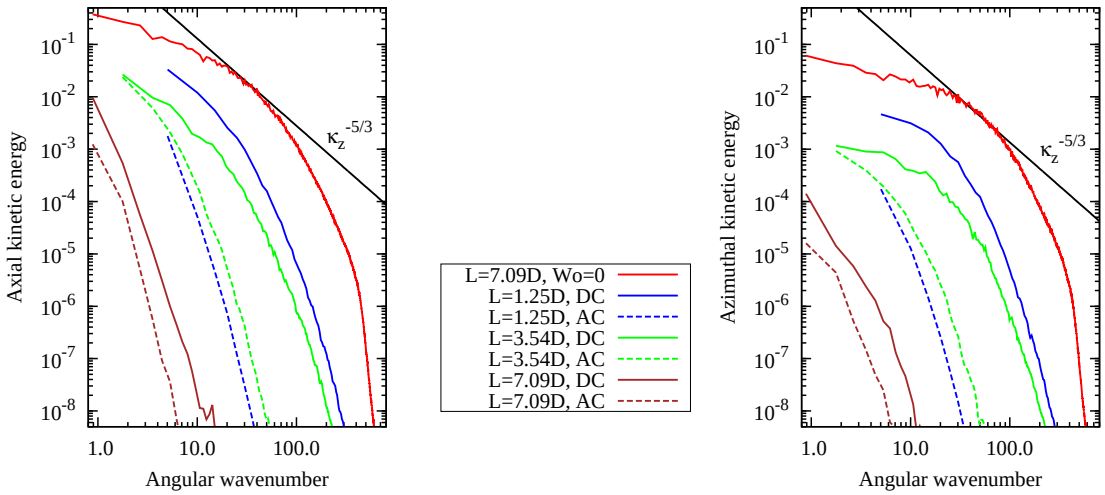

Figure 7. Axial energy spectra $\langle E_{z\alpha}(\kappa_z)\rangle_{\varphi,\phi}$ for the axial ($\alpha = z$, left) and the azimuthal ($\alpha = \varphi$, right) velocity component at a fixed radial position $r = 0.48$ averaged in azimuthal direction φ and over several equal oscillation phases ϕ, number of samples N_j and N_ϕ see table 1. Comparison for three different pipe length at phases of decelerating (DC) and accelerating (AC) bulk flow. Energy spectra for the fully developed non-oscillating pipe flow and a slope of $-5/3$ are shown for orientation.

energy from DC to AC in the shorter pipe domain.

CONCLUSIONS

We performed DNS of oscillating pipe flow at $Re = 11500$ and $Wo = 13$ using a fully developed turbulent flow field as initial condition. We found that for short and medium pipe domains, the flow is conditionally turbulent; characterised by an repeated amplification and damping of fluctuations. This is in accordance with qualitative descriptions of the flow field as found in experiments and also in former DNS for similar problems. Here, we focus on the influence of the length of the computational domain on the resulting flow field and found that the flow laminarises entirely and does not show an conditionally turbulent behaviour, when the computational domain exceeds a certain value. From our DNS we conclude, that the critical maximum pipe length for this special scenario lies within $3.54D < L_{\mathrm{crit}} < 5D$ and we propose an explanation for these observations by analysing spatial velocity spectra for different computational domain length.

For the cases, where a conditionally turbulent state is maintained, we have compared statistics and energy spectra, to quantify the influence of the domain length. As expected, we found only little influence of the pipe length on the integral quantities like bulk flow, wall shear stress and mean velocity profiles.

Comparing these quantities for the laminar and the turbulent flow fields, reveals major differences, which were not necessarily expected. For a given combination of Re and Wo, the peak flow rate is 4.5 % higher and at the same time the maximum shear forces acting on the wall are 4.8 % lower in case of a turbulent flow compared to a laminar flow in the same system.

References

Akhavan, R., Kamm, R. D. & Shapiro, A. H. 1991 An investigation of transition to turbulence in bounded oscillatory Stokes flows. *J. Fluid Mech.* **225**, 423–444.

Eckmann, D. M. & Grotberg, J. B. 1991 Experiments on transition to turbulence in oscillatory pipe flow. *J. Fluid Mech.* **222**, 329–350.

Eggels, J. G. M., Unger, F., Weiss, M. H., Westerweel, J., Adrian, R. J., Friedrich, R. & Nieuwstadt, F. T. M. 1994 Fully developed turbulent pipe flow: a comparison between direct numerical simulation and experiment. *J. Fluid Mech.* **268**, 175–210.

Feldmann, D. & Wagner, C. 2012 Direct numerical simulation of fully developed turbulent and oscillatory pipe flows at $\mathrm{Re}\tau = 1440$. *J. Turb.* **13** (32), 1–28.

Hino, M., Sawamoto, M. & Takasu, S. 1976 Experiments on transition to turbulence in an oscillatory pipe flow. *J. Fluid Mech.* **75** (2), 193–207.

Jiménez, J. & Moin, P. 1991 The minimal flow unit in near-wall turbulence. *J. Fluid Mech.* **225**, 213–240.

Sexl, T. 1930 Über den von E. G. Richardson entdeckten Annulareffekt. *Z Phy.* **61** (5-6), 349–362.

Spalart, P. R. & Baldwin, B. S. 1989 Direct Simulation of a Turbulent Oscillating Boundary Layer. *Turbulent Shear Flows* **6**, 417–440.

Thomas, C., Bassom, A. P. & Blennerhassett, P. J. 2012 The linear stability of oscillating pipe flow. *Phys. Fluids* **24** (1), 014106.

Trukenmüller, K. E. 2006 Stabilitätstheorie für die oszillierende Rohrströmung. Dissertation, Helmut-Schmidt-Universität, Hamburg.

Vittory, G. & Verzicco, R. 1998 Direct simulation of transition in an oscillatory boundary layer.

Womersley, J. R. 1955 Method for the calculation of velocity, rate of flow and viscous drag in arteries when the pressure gradient is known. *J. Physiol.* **127** (3), 553–563.

Zhao, T. S. & Cheng, P. 1996 Experimental studies on the onset of turbulence and frictional losses in an oscillatory turbulent pipe flow. *Int. J. Heat Fluid Fl.* **17** (4), 356–362.